Journal of Environmental Management 347 (2023) 119151

Contents lists available at ScienceDirect

Journal of Environmental Management

journal homepage: www.elsevier.com/locate/jenvman

Research article

Modeling the power system resilience in China under different natural disasters

Hao Chen [a,b], Kai Gong [a], Yunhao Chang [a], Weijun He [c,*], Haopeng Geng [d], Boyan Zhang [a], Wenfeng Zhang [a]

[a] School of Applied Economics, Renmin University of China, Beijing, 100872, China
[b] Department of Chemistry, Renmin University of China, Beijing, 100872, China
[c] School of Economics and Management, University of Science and Technology Beijing, Beijing, 100083, China
[d] School of Economics and Management, China University of Geosciences, Wuhan, 430074, China

ARTICLE INFO

Handling editor: Lixiao Zhang

Keywords:
Electricity system
Resilience
Natural disaster
Estimation
China

ABSTRACT

A good understanding of the power system resilience is necessary for optimizing the investment strategies and supporting the emergency rescue, but the existing quantitative estimation results based on real outage events are still lacked due to the data limitations. Therefore, this study first establishes a unified framework to measure the power system resilience under different natural disasters, by integrating the electricity performance curve with the dynamic inoperability input-output model. Then, a database of 285 Chinese historical big power outage events caused by natural disasters is established, and the city-level power system resilience values are estimated. Finally, a benefit analysis is conducted for improving the power system resilience. Our major findings are that: (1) Electricity system recoveries quickest from hail (23.05 h), while restores slowest from snowstorm (117.31 h). (2) China's city electricity system is the most resilient to the thunderstorm, while is the least resilient to the earthquake. (3) Enhancing the power system resilience will significantly reduce the requirements for rescue resources, and the saved emergency rescue cost ranges from 0.57 million yuan to 12.08 million yuan with 1% reduction of initial inoperability.

1. Introduction

Electricity supply infrastructure (ESI) is one of the lifelines of an economy, and its failures can affect the economic development and social stability greatly (Baik et al., 2020; Chen et al., 2022; Dugan et al., 2023; Perera et al., 2020). The direct economic losses from 2021 power outages caused by extreme weather in Texas were estimated to be more than $200 billion, while the South Africa's electricity crisis in 2023 was costing the economy as much as $51 million per day.[1] Various factors have caused large-scale blackouts during the past two decades, including natural disasters, equipment errors, human mistakes and balancing problems (see Fig. 1). With the changing climate caused by human activities, natural disasters are occurring more frequently and becoming a significant risk factor of power outages (Bhusal et al., 2020; Stott, 2016; Wu et al., 2022; Zhang et al., 2022a,b). Moreover, the affected population without electricity is typically higher under natural disasters when compared with other causing factors, which can be evidenced by the blackouts in Italy in 2003 and Brazil in 2009. Natural disasters can not only affect the electricity supply and demand, but also damage the ESI components (generators, grid lines and transformers) (Bollinger and Dijkema, 2016; Chen et al., 2021a). To reduce the economic loss from power outages, it is essential to have a good understanding of the power system resilience under different natural disasters, thus providing guidance for ESI investment strategies and strengthening the weak parts of the power system.

There are several challenges in analyzing the power system resilience under natural disasters. First, there is no clear and unified definition of the power system resilience under natural disasters, leading to

* Corresponding author. School of Economics and Management, University of Science and Technology Beijing, No.30 Xueyuan Road, Haidian District, Beijing, 100083, Beijing, PR China.

E-mail addresses: chenhao9133@126.com (H. Chen), gk2000@ruc.edu.cn (K. Gong), changyunhao@126.com (Y. Chang), whe0323@163.com (W. He), ghp926@cug.edu.cn (H. Geng), zhangboyan13@163.com (B. Zhang), wfzhang1217@126.com (W. Zhang).

[1] The data source for United States is from https://baijiahao.baidu.com/s?id=1726892905665240651&wfr=spider&for=pc. The data sources for South African is from https://www.bloomberg.com/news/articles/2023-02-06/blackouts-may-cost-s-africa-51-million-day-central-bank-says#xj4y7vzkg.

https://doi.org/10.1016/j.jenvman.2023.119151
Received 27 April 2023; Received in revised form 14 September 2023; Accepted 22 September 2023
Available online 28 September 2023
0301-4797/

inconsistency and incomparability of the assessment results (Panteli and Mancarella, 2015). Different disasters have different impact mechanisms, impact channels and impact levels on power outages, so a unified framework is needed to measure the power system resilience by integrating the common features of different natural disasters (Forzieri et al., 2018; Wender et al., 2017). Second, considering the significant heterogeneity of the outage events caused by different natural disasters, it is necessary to measure the resilience based on the detailed failure and recovery data of real outage events (Bollinger and Dijkema, 2016). However, the available database is still lacked due to the stochastic and unpredictable feature of power outages (Ji et al., 2016; Liu et al., 2021).

China has the largest electricity system in the world, whose electricity consumption accounts for 29% of the world in 2020 (BP, 2021). The scale of ESI also ranks top in the world, the total generation capacity is 2200 GW in 2020, while the total length of transmission and distribution lines is about 0.8 million km.[2] Due to the large land area and diverse topographical features, China is also one of the countries with a higher occurrence frequency of natural disasters (Wang et al., 2020). The overlap of big complex ESI with the frequent natural disasters makes the electricity system more vulnerable, thus affecting the stable operation of the electricity system (Chen et al., 2021a). In 2020, the system average interruption duration index (SAIDI) in China is 11.87 h, which is much higher than that of other developed countries (<1 h).[3] To further increase the electricity supply quality, it is necessary to assess the resilience of the electricity system. With this motivation, this study first develops an electricity resilience evaluation model under natural disasters, which combines the Dynamic inoperability input-output model (DIIM) and the electricity performance curve. Then, we collect 285 big city-level power outage events in China caused by six types of natural disasters (flood, snow and ice, thunderstorm, hail, earthquake and typhoon) from the news websites from 2005 to 2021, and then establish a database which contains the occurrence time, recovery time, causes, initial affected population, rescue workers and vehicles etc. After that, the resilience of city electricity system under different types of natural disasters is estimated, and a benefit analysis of enhancing the resilience of power system is conducted. During this process, we aim to answer the following three questions:

(1) What are the features of power outage events caused by natural disasters in China?
(2) What are the resilience levels of electricity system in different Chinese cities under different disasters?
(3) What are the benefits of improving China's power system resilience?

Compared with the previous studies, this study contributes to the literature from the following two aspects. First, an estimation model, integrating the DIIM model and electricity system performance curve, is developed to estimate the power system resilience, and the estimated results are comparable among different natural disasters. The DIIM model is employed to simulate the recovery trajectory of the electricity sector, while the performance curve is used to estimate the resilience index. Second, a database of historical big power outage events in China is established in this study, which will contribute to future related studies.

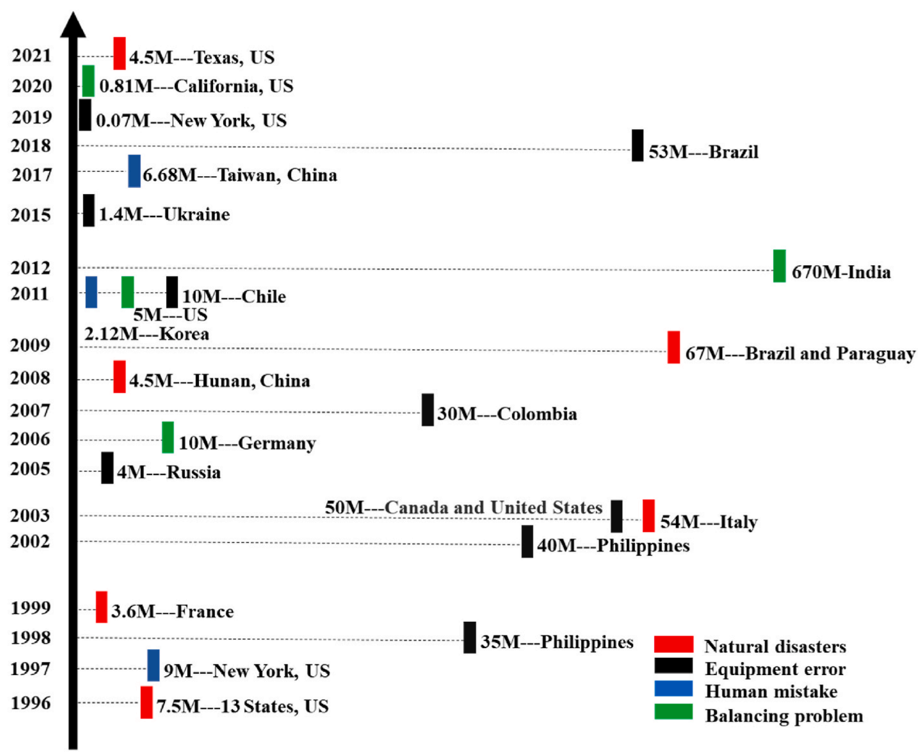

Fig. 1. Historical big outage events in the world
Notes; The horizontal axis shows the number of people affected by power outage events, and M represents one million people.

The remaining part of this paper is organized as follows: Section 2 presents the literature review, Section 3 shows the methodology and data used to assess the power system resilience, Section 4 describes the results and discussions, Section 5 summarizes the conclusions and proposes several policy implications.

[2] The data only includes the length of transmission lines above 220 kV. The data are drawn from the website of China Electricity Council, see https://cec.org.cn.
[3] The electricity reliability data of China is drawn from National Energy Administration, see http://www.nea.gov.cn/.

2. Literature review

Modern economy depends heavily on the safe and stable operation of electric power system (Chen et al., 2021b; Perera et al., 2020; Saurin and Júnior, 2011; Zhang et al., 2014). Understanding the power system resilience is a prerequisite for enhancing the electricity supply quality (Ouyang and Duenas-Osorio, 2014; Yusta et al., 2011). As the results of resilience estimation depend on the definition and the estimation method, this paper will review the existing literature in terms of these two topics.

The concept of resilience stemmed from material science, which refers to the ability of material to return to its original shape after deformation. Then, this concept of resilience was extended to other fields (biology, sociology, economics, engineering, infrastructure, etc) (Bollinger and Dijkema, 2016; Holling, 1973; Rieger, 2010; Summers et al., 2018). In 2009, the Unites States (US) Department of Energy (DOE) published a Smart Grid System Report and stated that smart grids should be resilient in the face of natural disasters, deliberate attacks, equipment failures and human errors (DOE, 2009). Inspired by the resilience description after earthquakes by Bruneau and Reinhorn (2007), Ouyang and Duenas-Osorio (2014) defined the power system resilience as '4R' (robustness, redundancy, resourcefulness and rapidity) in 2012. In 2015, the US Department of Homeland Security (DHS) defined resilience as the readiness and adaptation of a power system to deliberate attacks, accidents or natural disasters, and rapid recovery after experiencing a failure (DHS, 2013). Bie et al. (2015) pointed out that a resilient electricity system has three features. First, it has the ability to make corresponding preparations and preventions before the system encounters a disturbance event. Second, it has the ability to fully resist, absorb, respond and adapt when the system encounters a disturbance event. Third, it is able to quickly return to the preset expected normal state when the system encounters a disturbance event. There is no unified definition of the power system resilience, and the data used to measure it also varies significantly among different studies. The most frequent data used to assess the power system resilience include initial inoperability and recovery time (Haimes et al., 2005a; Poudineh and Jamasb, 2017; Wing and Rose, 2020).

The existing methods to estimate the power system resilience can be classified into three categories. The first one is a performance function curve approach. By comparing the actual electricity supply curve with the counterfactual business-as-usual supply curve, this approach defines the power system resilience as the ratio of the actual electricity output to the business-as-usual electricity output (Ouyang and Duenas-Osorio, 2014). Moreover, the popularly used models to describe electricity supply curve after outages include the trapezoid model and the triangle model (Bruneau and Reinhorn, 2007; Panteli et al., 2017). The second one is an inoperability input-output based approach. This approach was proposed by Haimes et al. (2005b), and could be used to analyze the inoperability and recovery of interdependent infrastructure system. Moreover, Lian and Haimes (2006) upgraded the original static inoperability input-output model to DIIM by considering the dynamic changes during the recovery process. This approach takes a macro perspective to analyze the performance of electricity sector by considering the dependence among different economic sectors. This model has an electricity resilience parameter and can be estimated empirically by using regression models. MacKenzie and Barker (2013) employed a regression model to estimate the electricity system resilience based on a DIIM. Poudineh and Jamasb (2017) employed an inoperability input-output model to assess business interruption costs from power outages in Scotland by considering the sectoral resilience. The third approach is a comprehensive evaluation method, which calculates a power system resilience index through weighted summation of different indicators. Reed et al. (2009) evaluated the power system resilience under extreme natural disaster events with consideration of the structural vulnerability. Molyneaux et al. (2012) evaluated the power system resilience in a range of Organization for Economic Co-operation and Development (OECD) and developing countries and examined their capability to cope with different natural shocks. Ouyang and Duenas-Osorio (2014) quantified the power system resilience under hurricane weather by building resilience metrics based on different composite indicators. Mensah and Dueñas-Osorio (2016) proposed an evaluation framework to quantify the power system resilience to hurricane events. World Bank (WB) has developed a set of indicators to measure the power system resilience under different hazards, including physical damage to power infrastructure, reduced supply of cooling water, shifts in peak flow, etc (WB, 2021). All the three approaches have advantages and drawbacks. The first approach is easy to use but have higher data requirements, and the hourly recovery data of power outage events is often not easy to be obtained (Liu et al., 2021). The third approach is more comprehensive, but it is a little subjective in both the indicator selection and the weight determination among different composite indicators. The second approach is more complex, but it can simulate the recovery path by considering the links among different sectors. Moreover, the DIIM model simulates the inoperability curves by considering the interdependency among different sectors. This is because natural disasters can affect different sectors simultaneously, and the inoperability of one sector can be transmitted to the other sectors (Poudineh and Jamasb, 2017). Considering our research targets and data availability, the DIIM model is very suitable for modeling the power system resilience under different natural disasters.

There are several gaps to be bridged in the existing literature. First, a unified framework is needed to measure the power system resilience and obtain comparable results for power system shocks from different types of natural disasters. Second, the recovery process depends on both the natural disaster shocks and power system resilience, and the recovery trajectory of the electricity sector needs to be simulated for estimating the power system resilience. Third, a database which collects information about previous power outage events is needed and can shed light on the future power system resilience studies.

3. Methodology

3.1. Power system resilience assessment model

This paper estimates the power system resilience based on the performance curve, which shows the dynamic changes of electricity sector inoperability after the occurrence of natural disasters. The inoperability measures the dysfunction of the electricity system and can be calculated as a share of the as-planned power supply, see equation (1).

$$q_i = \frac{x_i - \widetilde{x}_i}{x_i} \tag{1}$$

Where q_i is the inoperability of the electricity sector i; x_i is the as-planned power supply; $\widetilde{x}_i$ is the actual electricity supply after power outages. The value of q_i ranges from 0 to 1, and a lower value of q_i means a smaller impact on the electricity sector caused by the disaster.

With the occurrence of natural disasters, the inoperability of electricity sector will increase significantly from 0 to q(0). As the time goes by, the power system's inoperability will gradually decrease to 0 as the system recovers, see Fig. 2.

Based on the dynamic changes of power system inoperability, the power system resilience can be defined as the ratio of the post-disaster electricity supply to the total electricity supply under the business-as-usual scenario during the recovery period [t0, t1], see equation (2). The value of power system resilience index ranges from 0 to 1, and a higher index value indicates a better resilience of the power system.

$$ERI = \frac{(t_1 - t_0)\cdot 100\% - \int_{t_0}^{t_1} q(t)dt}{(t_1 - t_0)\cdot 100\%} \tag{2}$$

Although the resilience definition is easy to understand, the data of the electricity inoperability curve is not readily available. Therefore, a

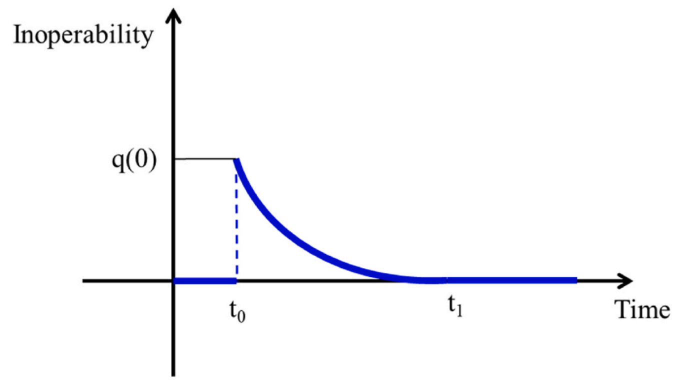

Fig. 2. The dynamic changes of electricity system inoperability after disaster occurrence.

dynamic inoperability input–output model is used to simulate the inoperability curve with consideration of the interdependencies among different sectors, then the economic losses can be estimated using the simulated inoperability curves and the sectoral economic output. The DIIM model is developed based on the traditional Input-Output analysis by introducing the inoperability, see equation (3).

$$\boldsymbol{x} = \boldsymbol{A}\boldsymbol{x} + \boldsymbol{c} \tag{3}$$

where $\boldsymbol{c} = [c_1, c_2, ..., c_n]^T$ is the demand vector of different sectors; $\boldsymbol{x} = [x_1, x_2, ..., x_n]^T$ indicates the total production of different sectors; $\boldsymbol{A} = [a_{ij}]_{n\times n}$ is the technology coefficient matrix which represents the input-output relationships between different sectors.

Equation (3) describes the input-output relationship between sectors under normal production conditions. When the natural disasters occur, production and consumption will fall to the level of $\widetilde{x}$ and $\widetilde{c}$ respectively, and the input-output relationship of the post-disaster economy can be expressed in equation (4).

$$\widetilde{\boldsymbol{x}} = \boldsymbol{A}\widetilde{\boldsymbol{x}} + \widetilde{\boldsymbol{c}} \tag{4}$$

Let equation (3) minus equation (4), and multiplying the diagonal matrix derived from vector $\boldsymbol{x}$ ($\widehat{\boldsymbol{x}}^{-1}$) on both sides, we can obtain the following equation.

$$\widehat{\boldsymbol{x}}^{-1}(\boldsymbol{x} - \widetilde{\boldsymbol{x}}) = \widehat{\boldsymbol{x}}^{-1}\boldsymbol{A}(\boldsymbol{x} - \widetilde{\boldsymbol{x}}) + \widehat{\boldsymbol{x}}^{-1}(\boldsymbol{c} - \widetilde{\boldsymbol{c}}) \tag{5}$$

equation (5) can be transformed to the static IIM equation (6).

$$\boldsymbol{q} = \boldsymbol{A}^*\boldsymbol{q} + \boldsymbol{c}^* \tag{6}$$

where

$$\mathbf{q} = \widehat{\mathbf{x}}^{-1}(\mathbf{x} - \widetilde{\mathbf{x}}) = \begin{bmatrix} \frac{1}{x_1} & 0 & \cdots & \cdots & 0 \\ 0 & \ddots & \ddots & \ddots & \vdots \\ \vdots & \ddots & \frac{1}{x_i} & \ddots & \vdots \\ \vdots & \ddots & \ddots & \ddots & 0 \\ 0 & \cdots & \cdots & 0 & \frac{1}{x_n} \end{bmatrix} \begin{bmatrix} x_1 - \widetilde{x}_1 \\ \cdots \\ x_i - \widetilde{x}_i \\ \cdots \\ x_n - \widetilde{x}_n \end{bmatrix} \tag{7}$$

$$\mathbf{A}^* = \widehat{\mathbf{x}}^{-1}\mathbf{A}\widehat{\mathbf{x}} = \begin{bmatrix} a_{11}\left(\frac{x_1}{x_1}\right) & \cdots & a_{1j}\left(\frac{x_j}{x_1}\right) & \cdots & a_{1n}\left(\frac{x_n}{x_1}\right) \\ \vdots & \ddots & \vdots & \ddots & \vdots \\ a_{i1}\left(\frac{x_1}{x_i}\right) & \ddots & a_{ij}\left(\frac{x_j}{x_i}\right) & \ddots & a_{in}\left(\frac{x_n}{x_i}\right) \\ \vdots & \ddots & \ddots & \ddots & \vdots \\ a_{n1}\left(\frac{x_1}{x_n}\right) & \cdots & a_{nj}\left(\frac{x_j}{x_n}\right) & \ddots & a_{nn}\left(\frac{x_n}{x_n}\right) \end{bmatrix} \tag{8}$$

$$\mathbf{c}^* = \widehat{\mathbf{x}}^{-1}(\mathbf{c} - \widetilde{\mathbf{c}}) = \begin{bmatrix} \frac{1}{x_1} & 0 & \cdots & \cdots & 0 \\ 0 & \ddots & \ddots & 0 & \vdots \\ \vdots & \ddots & \frac{1}{x_i} & \ddots & \vdots \\ \vdots & 0 & \ddots & \ddots & 0 \\ 0 & \cdots & \cdots & 0 & \frac{1}{x_n} \end{bmatrix} \begin{bmatrix} c_1 - \widetilde{c}_1 \\ \cdots \\ c_i - \widetilde{c}_i \\ \cdots \\ c_n - \widetilde{c}_n \end{bmatrix} \tag{9}$$

The DIIM model can be obtained by introducing the dynamic terms of sectoral inoperability and resiliency of the sectors to the static IIM, see equations (10) and (11). **K** is a resiliency matrix of different sectors during the recovery period when the disaster occurs

$$\mathbf{q}(\mathrm{t}+1) = \mathbf{q}(\mathrm{t}) + \mathbf{K}[\mathbf{A}^*\mathbf{q}(\mathrm{t}) + \mathbf{c}^*(\mathrm{t}) - \mathbf{q}(\mathrm{t})] \tag{10}$$

$$\dot{\mathbf{q}}(\mathrm{t}) = \mathbf{K}[\mathbf{A}^*\mathbf{q}(\mathrm{t}) + \mathbf{c}^*(\mathrm{t}) - \mathbf{q}(\mathrm{t})] \tag{11}$$

The differential equation in (11) has a general solution, as shown in equation (12).

$$\mathbf{q}(\mathrm{t}) = \mathbf{e}^{-\mathbf{K}(\mathbf{I}-\mathbf{A}^*)\mathrm{t}}\mathbf{q}(0) + \int_0^{\mathrm{t}} \mathbf{K}\mathbf{e}^{-\mathbf{K}(\mathbf{I}-\mathbf{A}^*)(\mathrm{t}-\mathrm{z})}\mathbf{c}^*(\mathrm{z})\mathrm{dz} \tag{12}$$

With the stationarity assumption of the final demand, $\mathbf{c}^* = 0$, we can obtain equation (13).

$$\mathbf{q}(\mathrm{t}) = \mathbf{e}^{-\mathbf{K}(\mathbf{I}-\mathbf{A}^*)\mathrm{t}}\mathbf{q}(0) \tag{13}$$

As can be seen from equation (13), the initial inoperability vector will fade off over time following the term $e^{-K(I-A^*)t}$. The recovery rate (k_i) of sector i can also be calculated based on equation (13) and the boundary condition at time t = 0 and t = T.

$$k_i = \frac{\ln[q_i(0)/q_i(T)]}{T_i(1 - a^*_{ii})} \tag{14}$$

Where $q_i(0)$ is the initial inoperability of the sector i caused by the natural disaster; T_i is the time when the sectoral inoperability level recovery to $q_i(T_i)$.

Using the empirically data from real power outage events, all the parameters in the DIIM model can be obtained. Then, the resilience index of the electricity sector (*ERI*) can be calculated based on the simulated inoperability curves, see equation (15). The index can be used to evaluate the power system resilience under different natural disasters, thus providing guidance for the weak parts strengthen and contributing to investment strategies of the power system.

$$ERI = \frac{(t_1 - t_0) - \int_{t_0}^{t_1} q(0)e^{-k(1-a^*)t}dt}{t_1 - t_0} = 1 + \frac{q(0)}{k(1-a^*)(t_1 - t_0)}\left[e^{-k(1-a^*)t_1} - e^{-k(1-a^*)t_0}\right] \tag{15}$$

3.2. Data

To bridge the gap of data unavailability in measuring the electricity system resilience, this study, to the best of our knowledge, is the first study to establish a database by collecting information of big natural disaster induced power outage events in China. The database includes 285 big power failure events occurred in different Chinese cities during the period from 2005 to 2021. Among them, the causes for power outages consist of flood (60 cases), snow and ice (40 cases), thunderstorm (48 cases), hail (47 cases), earthquake (40 cases) and typhoon (50 cases), as shown in Fig. 3. To support the electricity resilience analysis, we have collected the event cause, occurrence time, number of affected households, recovery time, number of emergency rescue workers and emergency rescue vehicles and other information for the power outage events.

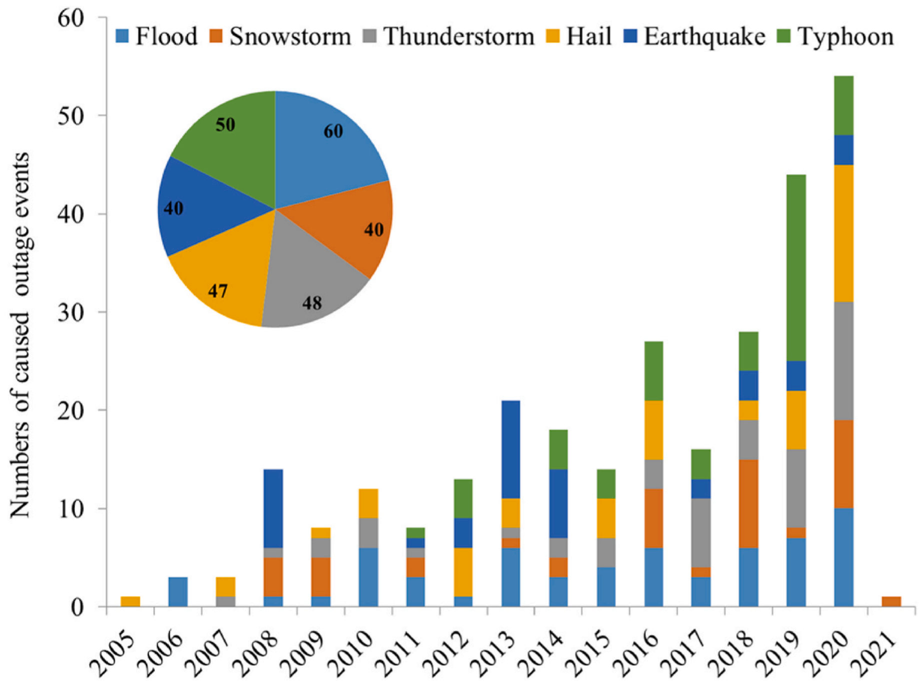

Fig. 3. The collected electricity outage events in this study
Notes: the list of these power outage events are obtained from the search engine widely used in China, namely Baidu (https://www.baidu.com/). The detailed information of these power outage events are mainly collected from Chinanews (https://www.chinanews.com/), NetEase News (https://news.163.com/), Sina News (https://news.sina.com.cn/), website of the meteorological department, such as China Typhoon website (http://typhoon.weather.com.cn/), China Earthquake Networks Center (https://news.ceic.ac.cn/).

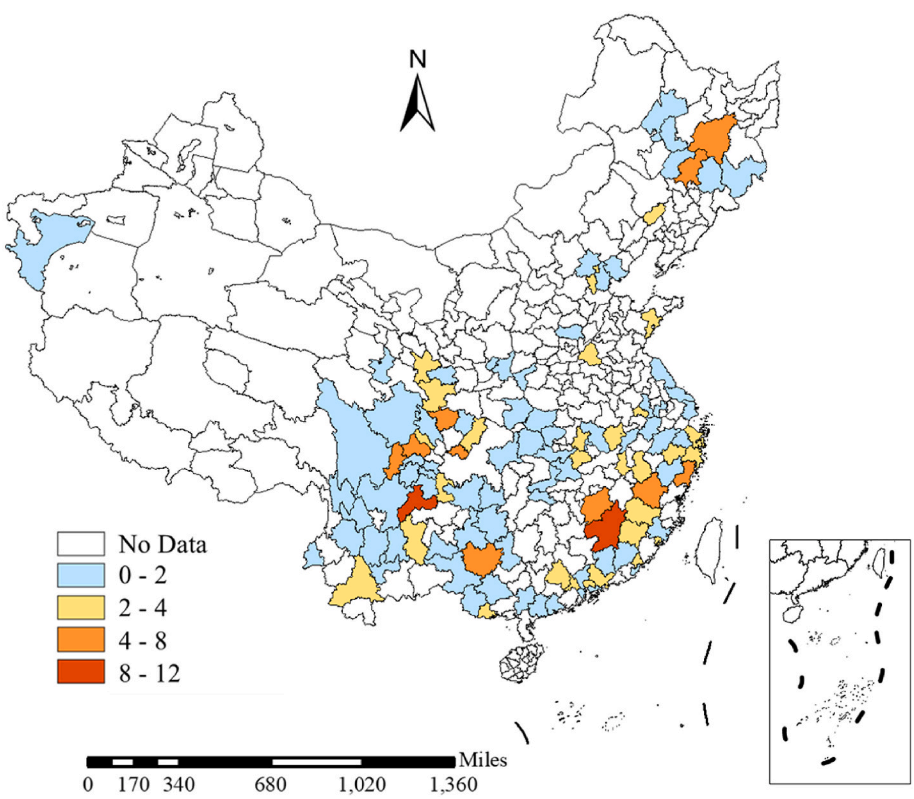

Fig. 4. The spatial distribution of electricity outage event numbers
Notes: All provincial boundaries are drawn from the Ministry of Civil Affairs of the People's Republic of China (http://xzqh.mca.gov.cn/map; map content approval number: GS(2023)2767).

As seen from Fig. 3, the number of power outage events caused by natural disasters shows a gradually rising trend during the sample period, exhibiting the importance to analyze the power system resilience with the accelerated climate change. The spatial distribution of power outage events are shown in Fig. 4, which shows the frequency of power outage events in different cities. As can be seen from Fig. 4, the southern China cities generally have higher frequency of power failure events than that in the northern China cities. There are two reasons to explain the spatial difference. On the one hand, the average annual rainfall in the southern China is significantly higher than that in the northern China, so the power systems in the southern cities are more vulnerable to floods, heavy rainfall and other disasters. The southern coastal cities are also more vulnerable to typhoons due to the influence of atmospheric circulation, which can cause serious damages to the ESI. The cities which experienced the largest number of power outage events are Ganzhou in Jiangxi province, Chengdu in Sichuan Province and Zhaotong in Yunnan province. All of them have experienced 8–12 times of power outage events during the study period, while the average number of power outages is 2.5 in the sampled cities. With a good understanding of the pattern and spatial distribution of the historical power outages, more targeted measures can be taken to enhance the power system resilience.

To model the power system resilience in China under different natural disasters, the major input parameters for the DIIM model are the recovery time, the initial inoperability, the final inoperability, the interdependency matrix A*and the sectoral economic outputs. The sources and explanations are described as below.

Based on the power outage database established by us, the inoperability of the electricity sector is calculated as the share of interrupted households in the total number of households within a city during a power outage event. The recovery time is also directly drawn from the database, which is the duration between the start time and end time of a power outage event. Moreover, its unit is measured in hours. The final inoperability is set as $10^{-8}$with reference to Chen et al. (2022). The interdependency matrix A* is calculated based on the national Input-Output (I–O) table published by National Bureau of Statistics (NBS), and the calculation process can be seen from equation (8). The sectoral economic outputs are drawn from National Bureau of Statistics (NBS).

4. Results and discussions

4.1. Statistical analysis of the power outage events

To grasp the features of power outage events caused by natural disasters in China, we first conduct a statistical analysis of these outage events collected in the database. The temporal distribution of the starting time of power outage events is shown in Fig. 5. The first row shows the 24 h during a typical day, while the first column presents the provincial names in China. The numbers in the cells indicate the numbers of outage events occurred in the province during the specified hour, while the numbers on the right hand side column and in the bottom row show the total number of power outage events. As can be seen from Fig. 5, the most frequent time of disaster-induced power outages is concentrated in the evening and the early morning, especially at 1:00 and at 21:00. These time periods are the rest and sleep time for most Chinese people, resulting in challenges for the power system rescue.

The occurrence time of electricity outage events are also compared among different natural disasters, see Fig. 6. There are significant

	1	2	3	4	5	6	7	8	9	10	11	12	13	14	15	16	17	18	19	20	21	22	23	24	
Beijing	0	0	0	0	0	0	0	0	0	0	1	0	0	0	1	0	0	0	0	0	0	0	0	0	**2**
Tianjin	0	0	0	0	0	0	0	0	0	0	0	0	0	0	0	0	0	0	0	0	0	0	1	0	**1**
Hebei	0	0	0	0	0	0	0	0	0	0	0	0	0	0	0	0	0	1	0	0	1	1	1	0	**4**
Shanxi	0	0	0	0	0	0	0	0	0	0	0	0	0	0	0	0	0	0	0	0	0	0	0	0	**0**
liaoning	0	0	0	0	0	0	0	0	0	0	0	1	0	0	0	0	0	0	0	0	1	0	1	0	**3**
Jilin	0	0	1	0	0	0	0	0	0	0	0	0	0	0	0	0	1	0	3	0	0	0	0	0	**5**
Heilongjiang	2	0	0	0	0	0	0	1	0	0	0	0	0	0	0	0	0	1	1	1	0	2	0	0	**8**
Jiangsu	0	4	0	0	0	0	0	0	0	1	0	0	0	0	1	0	0	0	0	0	1	0	1	0	**8**
Shanghai	0	1	0	0	0	0	0	0	0	0	0	0	1	0	0	0	0	0	0	0	0	0	0	0	**2**
Zhejiang	0	4	1	4	1	0	0	0	0	0	0	0	0	1	0	0	1	2	0	0	3	1	0	0	**18**
Anhui	0	2	0	0	0	0	0	1	0	0	0	0	0	1	0	1	0	0	0	0	1	0	0	0	**6**
Fujian	0	1	0	5	0	0	1	0	1	0	0	0	0	1	0	0	0	3	0	0	1	0	0	0	**13**
Jiangxi	2	0	0	0	1	0	0	1	0	0	0	0	0	0	0	1	0	0	1	0	1	0	1	0	**8**
Shandong	0	0	0	0	0	0	1	0	5	0	0	0	0	0	0	0	0	0	0	0	0	0	0	0	**6**
Henan	0	0	0	0	0	0	0	0	0	0	0	0	0	0	0	0	0	0	0	0	0	0	0	0	**0**
Hubei	3	0	2	1	0	0	0	0	1	0	1	0	0	0	0	1	0	0	1	0	1	1	0	0	**12**
Hunan	0	0	0	0	0	0	0	1	0	0	0	0	0	0	0	0	1	0	0	0	1	0	0	0	**3**
Guangdong	0	0	0	0	0	0	0	0	0	1	2	0	2	0	1	0	1	3	0	3	1	2	0	0	**16**
Guangxi	2	0	0	0	0	0	0	1	0	1	0	0	0	0	2	1	0	0	1	0	5	0	0	0	**13**
Hainan	0	0	0	0	0	0	0	0	0	0	0	0	0	0	0	0	0	0	0	0	0	0	0	0	**0**
Sichuan	7	0	0	0	0	1	1	1	2	0	0	0	1	1	5	0	1	0	0	1	3	0	1	2	**27**
Guizhou	0	0	0	0	0	0	0	0	0	0	0	0	0	1	0	0	0	0	0	1	0	1	0	1	**4**
Yunnan	0	1	0	0	1	0	0	0	1	0	1	1	1	0	0	2	3	0	1	1	1	4	0	0	**18**
Chongqing	1	0	0	0	0	0	0	0	0	2	0	0	0	0	0	0	0	0	0	0	0	0	0	2	**5**
Shaanxi	0	0	0	0	0	0	0	0	0	0	0	0	0	0	0	0	1	0	0	0	0	0	0	1	**2**
Gansu	0	0	0	0	0	0	0	1	0	0	0	0	0	0	1	0	0	2	0	0	0	1	0	0	**5**
Qinghai	0	0	1	0	0	0	0	0	0	0	0	0	0	0	0	0	0	0	0	0	0	0	0	0	**1**
InnerMon.	0	0	0	0	0	0	0	0	0	0	0	0	0	0	0	0	0	0	0	0	0	0	0	0	**0**
Tibet	0	0	0	0	0	0	0	0	0	0	0	0	0	0	0	0	0	0	0	0	0	0	0	0	**0**
Ningxia	0	0	0	0	0	0	0	0	0	0	0	0	0	0	0	0	0	0	0	0	0	0	0	0	**0**
Xinjiang	0	0	0	0	0	0	0	0	0	0	0	0	0	0	0	0	0	0	0	0	0	1	0	0	**1**
	17	**13**	**5**	**10**	**3**	**1**	**3**	**7**	**10**	**5**	**5**	**2**	**5**	**5**	**11**	**6**	**9**	**12**	**8**	**7**	**21**	**14**	**6**	**6**	

Fig. 5. The occurrence time of electricity outage events in different provinces
Notes:Due to limited data availability, only 191 blackout events are included in this figure.

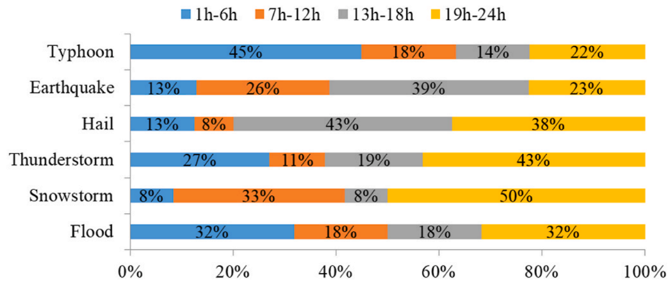

Fig. 6. The share of outage occurrence time under different natural disasters [191].

differences among these six disasters. Flood induced power outages tend to occur in the late afternoon and in the early morning, typhoon caused power outages tend to happen in the early morning, earthquake and hail caused power outages tend to occur in the afternoon, thunderstorm, ice and snow induced power outages tend to happen in the evening.

The total household number affected by disaster-induced power outages are shown in Fig. 7. The average number of affected households under different disasters varies significantly. Typhoon, on average, causes the largest number of households (716,400) without electricity, while thunderstorm affects the smallest number of households (72,600). Therefore, more attention should be paid to the types of disasters that have larger impacts.

The recovery time of power outage events under different natural disasters are compared in Fig. 8. The average recovery time exhibits a descending order from left to right. We can see that snowstorm caused power outages have the longest average recovery time (117.31 h), while the hail induced power outages have the smallest average recovery time (23.05 h). The large disparities attest to the heterogeneity in the recovery time under different disasters.

In addition, some interesting results can be obtained from the comparison between Figs. 7 and 8. First, there is an inconsistency between the number of people affected and the recovery time. For example, the typhoon induced power outages has the largest affected population, but its recovery time length ranks only fifth among these six disasters. Second, more attention should be paid to the disaster types which have both relatively larger number of affected households and recovery time, such as snowstorm and earthquake.

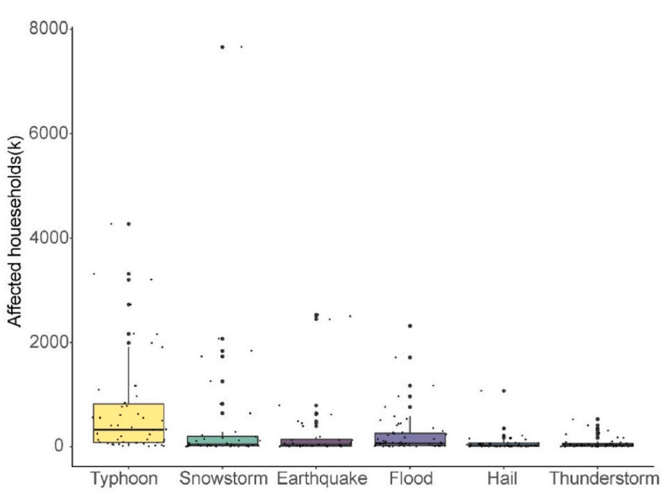

Fig. 7. The number of affected households with the occurrence of power outages

Notes: every dot in the chart indicates the affected households in a power outage event.

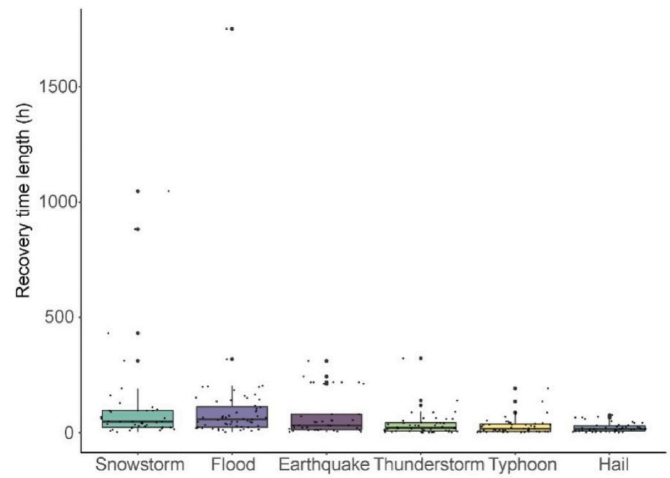

Fig. 8. The length of recovery time after power outages

Notes: every dot in the chart indicates the recovery time in a power outage event.

4.2. Resilience estimation under different natural disasters

Based on the model established in section 3, the electricity system resilience under six types of natural disasters is estimated at the city level and shown in Fig. 9. We can see that the places where the power outage events occur vary significantly among the six disasters. For example, the typhoon has the most serious impact on coastal cities, while the earthquake mainly influences the cities in the western provinces. The estimated city-level resilience values are marked with different colors in Fig. 9, and a darker color indicates a bigger resilience value of the city electricity system. We can see that the resilience levels differ among different cities under the same disaster. Taken the electricity system resilience under flood disaster in Yunnan province as an example, we can see that it has covered three resilience levels in the same province. The estimated resilience values can be compared not only within the same disaster type, but also be compared among different types of disasters. Therefore, the estimated resilience values can help identify the weak parts of the electricity system under different natural disasters. In addition, they can also be served as a tool to compare the resilience level of electricity system, thus providing support for the electricity reliability policies.

Notes:the resilience values of the city are the average values of the all the power outage events occurred in the same city in the database. All provincial boundaries are drawn from the Ministry of Civil Affairs of the People's Republic of China (http://xzqh.mca.gov.cn/map; map content approval number: GS(2023)2767).

In addition, we have also compared the average values of China's city-level power system resilience under different disaster types, see Fig. 10. We can see that China's city electricity system is the most resilient to the thunderstorms, while is the least resilient to the earthquakes. Moreover, the average resilience values are very high (>0.99) among all the six types of natural disasters, indicating that the city-level electricity system is very resilient to the shocks of natural disasters. This is because the number of initial affected households is still very small when compared with the total number of households at the city level. However, the estimated resilience values will be smaller if smaller administrative area is used in the resilience estimation, such as the county-level power system or the village-level power system. The comparison among different resilience values is meaningful, because the weak parts of the spatial electricity system or the large influencing disasters can be identified.

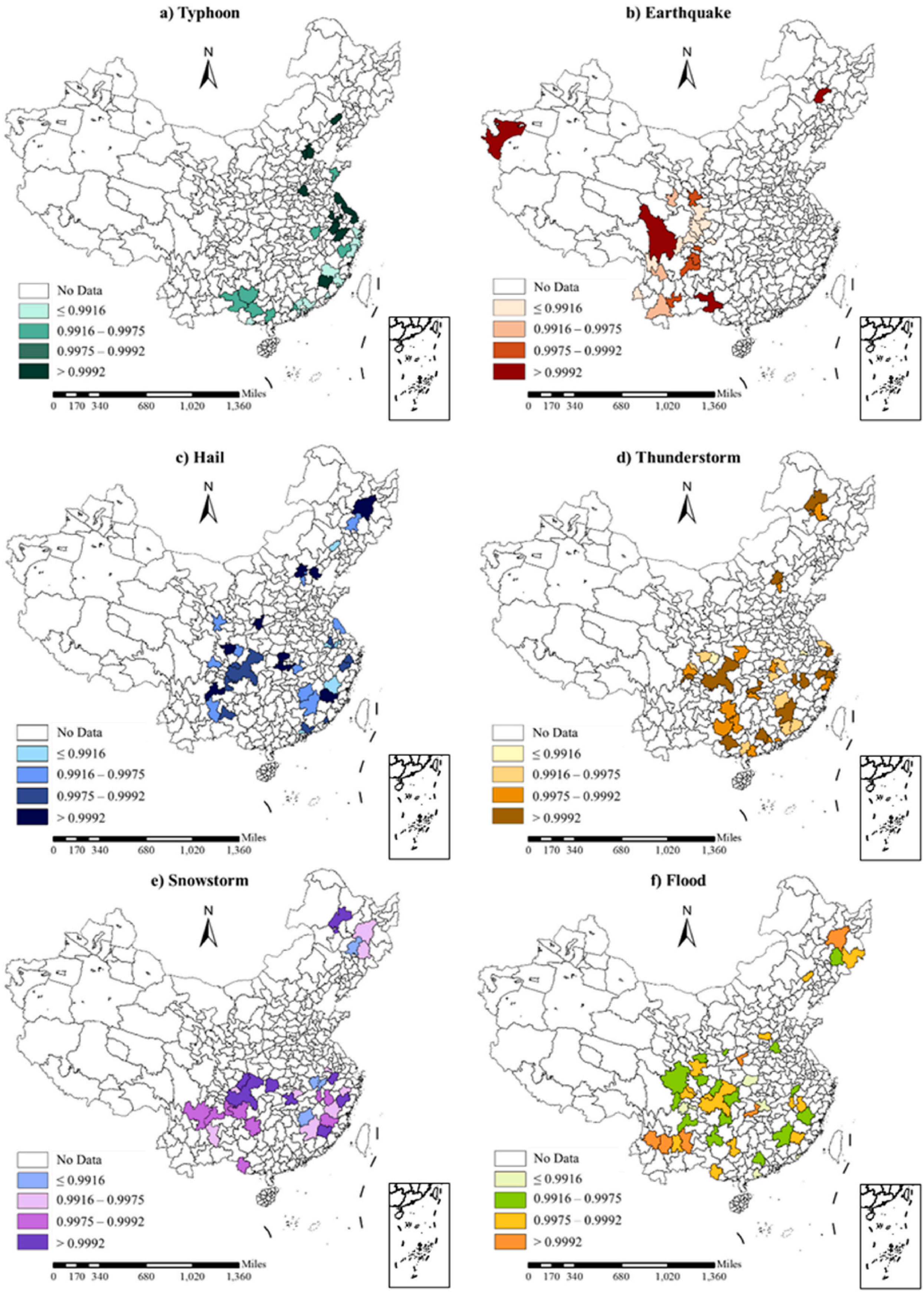

Fig. 9. The resilience index of city-level electricity system under different natural disasters.

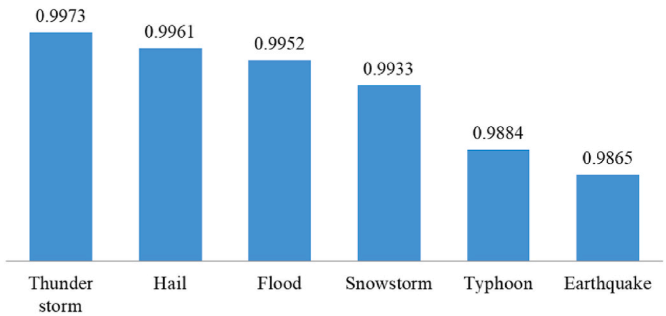

Fig. 10. The average resilience index of electricity system under different natural disasters.

4.3. The impacts of enhancing power system resilience on the emergency rescue cost

Once the resilience levels of the city electricity system are obtained, it is necessary to understand the benefits of enhancing the power system resilience. To illustrate the impacts of resilience enhancement on the power system operation cost reductions, this section analyzes the impacts of initial power system inoperability on the number of needed repair workers and emergency rescue vehicles. A more resilient city electricity system will have less initial inoperability, thus reducing the demand for emergency rescue resources. Table 1 shows the influences of initial inoperability on the number of repair workers under six types of natural disasters. The initial inoperability has significant impacts on the repair workers at the 10% significance level in all the natural disasters except the thunder storm. Moreover, the initial inoperability caused by typhoon has the largest impacts. The number of emergency rescue people will, on average, increase by 241 people when the initial inoperability increases by 1%. The initial inoperability caused by thunderstorm does not seem to have any significant impact on the number of repair workers. This is because the impacts on the electricity supply infrastructure vary among different types of natural disasters. Most of the existing electricity supply infrastructure has already installed lightning protection measures, so the thunder storm has relatively small physical damage impacts on the generators, transmission lines and transformer substations. Moreover, the breadth and depth of thunderstorm impact on electricity supply infrastructure is relatively smaller when compared with other types of natural disaster, so the number of needed emergency rescue people is smaller. Moreover, the R square is also very small, indicating a not very good fitness. This is mainly because the existing ESI has already been equipped with the thunder-storm resists tools, and has a certain degree of self-healing ability (Watson et al., 2021).

The impacts of initial inoperability on the emergency rescue vehicles are also investigated and shown in Table 2. We can see that the initial inoperability has significant impacts on the emergency rescue vehicles in most of the natural disaster induced power outages. The impacts of earthquake on the emergency rescue vehicles are the largest. The emergency rescue vehicles will, on average, increase by 82 when the initial inoperability increases by 1%. The impacts of hail on the emergency rescue vehicles are the smallest, each 1% increase in the initial inoperability will need 12 additional emergency vehicles. Similar to the impacts on emergency rescue people, the impacts on emergency rescue vehicles vary among different disasters. This is because different types of natural disasters have different impacts on the power outage length and affected people, and the major function of emergency rescue vehicles are used to supply electricity during the recovery process. Take the power outage after earthquakes as an example, more people and wide land area will be affected, so a larger number of emergency rescue vehicles are put into use to guarantee the most basic life of residents.

According to the State Grid Corporation of China (SGCC), the average cost of repair workers and emergency vehicles are 500 yuan/day and 46,000 yuan/day respectively in 2018 (SGCC, 2017). Based on the estimated impacts from initial inoperability reductions, we can assess how the enhancement of the electricity system resilience (1% reductions of initial inoperability) will affect the emergency rescue cost, as shown in Table 3. We can see that 1% of the reductions of initial inoperability will save the rescue cost by 0.57–12.08 million yuan. The average cost reductions are 4.54 million yuan for every 1% reductions of the initial inoperability. Moreover, the power outages caused by earthquake have the largest cost reductions, while the power outages induced by hail have the least cost reductions. These results can provide a reference for decision making in the cost-benefit analysis of power system resilience improvement.

5. Conclusions and policy implications

5.1. Conclusions

Natural disaster is one of the important factors affecting the reliable electricity supply in China, and many big blackouts are caused by different types of natural disasters in the history. To achieve a more resilient electricity system to natural disasters, it is necessary to have a good understanding of the electricity system resilience. With this motivation, this study first establishes a unified framework to estimate the power system resilience under different natural disasters, by integrating the electricity performance curve with the DIIM model. Then, a database of 285 Chinese historical big power outage events caused by natural disasters is established, and the city-level power system resilience is estimated based on the database. Finally, a benefit analysis is conducted for increasing the resilience of the power system. During this process, we have achieved the following conclusions:

(1) Due to the unique feature of power outages caused by different types of disasters, more targeted policies should be designed to monitor and defend against power outages caused by natural disasters. Taken the occurrence time as an example, the most frequent occurrence period of power outages events differs among different disasters. Typhoon caused power outages tend to happen in the early morning, while snowstorm induced power outages are inclined to occur in the late evening. Therefore, the allocation of emergency rescue resources can be optimized with consideration of the disaster heterogeneity, thus reducing the adverse impacts on the economic system.
(2) Statistical information of previous power outages is important for understanding the impacts and characteristics of different

Table 1
The impacts of initial inoperability on the repair workers.

Disasters	Typhoon	Snowstorm	Earthquake	Flood	Hail	Thunder storm
q(0)	24,134.39* (12,017.48)	13,183.27*** (4284.83)	14,175.30** (6286.07)	11,986.86** (4444.23)	11,158.71*** (2868.18)	10,671.15 (8291.05)
Constant	5765.60** (2112.43)	605.49* (305.59)	420.38* (216.76)	749.59*** (254.56)	298.14** (106.67)	493.05** (184.83)
Observations	17	15	16	19	13	14
R-squared	0.21	0.42	0.27	0.30	0.58	0.12

Note:The numbers in the small brackets are the standard errors, ***$p < 0.01$, **$p < 0.05$, *$p < 0.1$. Due to the limited information of the rescue workers, the observations are smaller than the total number of the power outage events.

Table 2
The impacts of initial inoperability on the emergency rescue vehicles.

Disasters	Typhoon	Snowstorm	Earthquake	Flood	Hail	Thunder storm
q(0)	3287.11** (1153.61)	1713.82* (851.19)	8229.93*** (886.65)	3424.15*** (786.73)	1157.80** (431.32)	1624.25 (1081.99)
Constant	552.04** (202.78)	154.92** (60.71)	−39.00 (30.57)	93.16* (45.06)	29.32* (16.04)	148.10*** (24.12)
Observations	17	15	16	19	13	14
R-squared	0.35	0.24	0.86	0.52	0.40	0.16

Note:The numbers in the small brackets are the standard errors, ***$p < 0.01$, **$p < 0.05$, *$p < 0.1$. Due to the limited information of the rescue vehicles, the observations are smaller than the total number of the power outage events.

Table 3
The impacts of 1% reduction of the initial inoperability on the emergency rescue cost.

Type	Typhoon	Snowstorm	Earthquake	Flood	Hail	Thunderstorm
Repair workers	241.34	131.83	141.75	119.86	111.58	106.71
Emergency vehicles	32.87	17.13	82.29	34.24	11.57	16.24
Recovery time (h)	29.93	117.31	75.20	104.43	23.50	37.74
Reduced cost (M. yuan)	2.04	4.18	12.08	7.11	0.57	1.26

disasters, thus contributing to a better design of the electricity reliability policies and rescue strategies. Among the six types of natural disaster induced power outages, typhoon affects the largest average number of households (716,400), while thunderstorm influences the smallest number of households (72,600). Moreover, electricity system recoveries quickest from hail (23.05 h), while restores slowest from snowstorm (117.31 h).

(3) China's city-level electricity system is relatively resilient to the natural disasters, and the comparison among different resilience values can help identifying the weak parts of the spatial electricity system. Differences exist among the resilience levels of electricity system in the face of the natural disasters. China's city electricity system is the most resilient to the thunderstorm, while is the least resilient to the earthquake.

(4) Enhancing the power system resilience will significantly reduce the requirements for rescue resources, no matter for the repair workers or the emergency rescue vehicles. Among the six natural disasters, the 1% reduction of initial inoperability will have the largest impacts on the repair worker requirements under typhoon disaster, while have the largest influences on the rescue vehicle requirements under earthquake disaster. Moreover, the saved emergency rescue cost ranges from 0.57 million yuan to 12.08 million yuan with 1% reduction of initial inoperability.

5.2. Policy implications

Based on the achieved conclusions, we have proposed the following policy implications to better improve the power system resilience in the future:

First, the estimated city-level electricity resilience results can be used as a tool to compare the resilience among different cities and identify the weak parts for future ESI investment. Therefore, it is necessary for the government to help establish a platform to dynamically monitor the power system resilience in different cities in China. With the platform, the investment resources can be allocated more wisely to the less resilient cities, enabling a stronger and more reliable electricity supply in China.

Second, a database of natural disaster induced power outages is of great significance in both preventing the outage occurrence and scheduling the emergency rescue activities. This study has pioneered in establishing a database of city-level power outages in China. Although the number of outage events contained in this study is still not big, the indicators (occurrence time, recovery time and affected population, etc) are very valuable in supporting the decisions making in the electricity reliability policies. It is beneficial for the government to make more information of disaster-induced outage publicly available, thus providing more in-depth understanding of the impacts and features of power outages in China.

Third, the emergency rescue resources for power outages can be saved when the electricity system become more resilient. A scientific plan for the allocation of emergency rescue resources is important for reducing the adverse impacts of power outages. The government can integrate the impacts of resilience into the electricity system emergency rescue plan, thus making more timely and cost-effective decisions in the rescue activities.

Although this paper has answered several important questions regarding the power system resilience, some improvements can be done in future studies. First, more power outage events can be added to the database, based on which more information can be provided for understanding the power system resilience. Second, this study only estimates the partial benefits from reducing the initial inoperability of electricity system, more benefits can be included when the data are available in the future. Third, the scale of the disasters can be considered in the resilience estimation, which can provide more details of the disaster impacts and corresponding power system responses. With these improvements done, a better understanding of the power system resilience can be achieved in the future.

CRediT authorship contribution statement

Hao Chen: Conceptualization, Methodology, Writing – original draft. **Kai Gong:** Software, Data collection, Writing – review & editing. **Yunhao Chang:** Methodology, Data curation, Visualization. **Weijun He:** Methodology, Writing – review & editing. **Haopeng Geng:** Methodology, Data curation, Visualization. **Boyan Zhang:** Writing – review & editing. **Wenfeng Zhang:** Data collection, Software.

Declaration of competing interest

The authors declare that they have no known competing financial interests or personal relationships that could have appeared to influence the work reported in this paper.

Data availability

Data will be made available on request.

Acknowledgement

This work was supported by the National Natural Science Foundation of China [grant number 72274198, 71904180, 72141308], the Ministry of Education Humanities and Social Sciences Foundation Youth Project [grant number 19YJC630008]. The authors would also like to extend a special thanks to the editor and the anonymous reviewers for their constructive comments and suggestions, which improved the quality of this article.

References

Baik, S., Davis, A.L., Park, J.W., Sirinterlikci, S., Morgan, M.G., 2020. Estimating what US residential customers are willing to pay for resilience to large electricity outages of long duration. Nat. Energy 5, 250–258.

Bhusal, N., Gautam, M., Abdelmalak, M., Benidris, M., 2020. Modeling of Natural Disasters and Extreme Events for Power System Resilience Enhancement and Evaluation Methods, 2020 International Conference on Probabilistic Methods Applied to Power Systems (PMAPS). IEEE, pp. 1–6.

Bie, C., Lin, Y., Qiu, A., 2015. Basic concepts and research prospects of resilient power grid and its resilience. Autom. Electr. Power Syst. 1–9 (in Chinese).

Bollinger, L.A., Dijkema, G.P., 2016. Evaluating infrastructure resilience to extreme weather–the case of the Dutch electricity transmission network. Eur. J. Transport Infrastruct. Res. 16, 214–239.

BP, 2021. BP Statistical of World Energy. Available at: https://www.bp.com.

Bruneau, M., Reinhorn, A., 2007. Exploring the concept of seismic resilience for acute care facilities. Earthq. Spectra 23, 41–62.

Chen, H., Liu, S., Liu, Q., Shi, X., Wei, W., Han, R., Küfeoğlu, S., 2021a. Estimating the impacts of climate change on electricity supply infrastructure: a case study of China. Energy Pol. 150, 112–119.

Chen, H., Yan, H., Gong, K., Geng, H., Yuan, X.-C., 2022. Assessing the business interruption costs from power outages in China. Energy Econ. 105, 105757.

Chen, H., Yan, H., Gong, K., Yuan, X.C., 2021b. How will climate change affect the peak electricity load? Evidence from China. J. Clean. Prod. 322, 1–14.

DHS, 2013. Critical Infrastructure Security and Resilience Functional Relationships. Department of Homeland Security, Washington DC. Available at: https://www.aga.org.

DOE, 2009. 2009 Smart Grid System Report. US Department of Energy, Washington DC. Available at: https://www.energy.gov/oe/downloads/2009-smart-grid-system-report-july-2009.

Dugan, J., Byles, D., Mohagheghi, S., 2023. Social vulnerability to long-duration power outages. Int. J. Disaster Risk Reduc. 85, 103501.

Forzieri, G., Bianchi, A., Silva, F.B., Herrera, M.A.M., Leblois, A., Lavalle, C., Aerts, J.C., Feyen, L., 2018. Escalating impacts of climate extremes on critical infrastructures in Europe. Global Environ. Change 48, 97–107.

Haimes, Y.Y., Horowitz, B.M., Lambert, J.H., Santos, J., Crowther, K., Lian, C., 2005a. Inoperability input-output model for interdependent infrastructure sectors. II: case studies. J. Infrastruct. Syst. 11, 80–92.

Haimes, Y.Y., Horowitz, B.M., Lambert, J.H., Santos, J.R., Lian, C., Crowther, K.G., 2005b. Inoperability input-output model for interdependent infrastructure sectors. I: theory and methodology. J. Infrastruct. Syst. 11, 67–79.

Holling, C.S., 1973. Resilience and stability of ecological systems. Annu. Rev. Ecol. Systemat. 4, 1–23.

Ji, C., Wei, Y., Mei, H., Calzada, J., Carey, M., Church, S., Hayes, T., Nugent, B., Stella, G., Wallace, M., 2016. Large-scale data analysis of power grid resilience across multiple US service regions. Nat. Energy 1, 1–8.

Lian, C., Haimes, Y.Y., 2006. Managing the risk of terrorism to interdependent infrastructure systems through the dynamic inoperability input–output model. Syst. Eng. 9, 241–258.

Liu, H., Tatano, H., Kajitani, Y., 2021. Estimating lifeline resilience factors using post-disaster business recovery data. Earthq. Spectra 37, 567–586.

MacKenzie, C.A., Barker, K., 2013. Empirical data and regression analysis for estimation of infrastructure resilience with application to electric power outages. J. Infrastruct. Syst. 19, 25–35.

Mensah, A.F., Dueñas-Osorio, L., 2016. Efficient resilience assessment framework for electric power systems affected by hurricane events. J. Struct. Eng. 142, 1–13.

Molyneaux, L., Wagner, L., Froome, C., Foster, J., 2012. Resilience and electricity systems: a comparative analysis. Energy Pol. 47, 188–201.

Ouyang, M., Duenas-Osorio, L., 2014. Multi-dimensional hurricane resilience assessment of electric power systems. Struct. Saf. 48, 15–24.

Panteli, M., Mancarella, P., 2015. Influence of extreme weather and climate change on the resilience of power systems: impacts and possible mitigation strategies. Elec. Power Syst. Res. 127, 259–270.

Panteli, M., Mancarella, P., Trakas, D.N., Kyriakides, E., Hatziargyriou, N.D., 2017. Metrics and quantification of operational and infrastructure resilience in power systems. IEEE Trans. Power Syst. 32, 4732–4742.

Perera, A., Nik, V.M., Chen, D., Scartezzini, J.L., Hong, T., 2020. Quantifying the impacts of climate change and extreme climate events on energy systems. Nat. Energy 5, 150–159.

Poudineh, R., Jamasb, T., 2017. Electricity supply interruptions: sectoral interdependencies and the cost of energy not served for the Scottish economy. Energy J. 38, 51–76.

Reed, D.A., Kapur, K.C., Christie, R.D., 2009. Methodology for assessing the resilience of networked infrastructure. IEEE Syst. J. 3, 174–180.

Rieger, C.G., 2010. Notional examples and benchmark aspects of a resilient control system, 2010 3rd International symposium on resilient control systems. IEEE 64–71.

Saurin, T.A., Júnior, G.C.C., 2011. Evaluation and improvement of a method for assessing HSMS from the resilience engineering perspective: a case study of an electricity distributor. Saf. Sci. 49, 355–368.

SGCC, 2017. Guidebook for The Maintenance and Operation Cost of State Grid Corporation of China. Available at: http://www.sgcc.com.cn/.

Stott, P., 2016. How climate change affects extreme weather events. Science 352, 1517–1518.

Summers, J.K., Harwell, L.C., Smith, L.M., Buck, K.D., 2018. Measuring community resilience to natural hazards: the natural hazard resilience screening index (NaHRSI)—development and application to the United States. GeoHealth 2, 372–394.

Wang, Q., Zhang, Q.-P., Liu, Y.-Y., Tong, L.-J., Zhang, Y.-Z., Li, X.-Y., Li, J.-L., 2020. Characterizing the spatial distribution of typical natural disaster vulnerability in China from 2010 to 2017. Nat. Hazards 100, 3–15.

Watson, P.L., Koukoula, M., Anagnostou, E., 2021. Influence of the characteristics of weather information in a thunderstorm-related power outage prediction system. Forecasting 3, 541–560.

WB, 2021. Resilience Rating System: A Methodology for Building and Tracking Resilience to Climate Change. World Bank. https://www.worldbank.org/en/home.

Wender, B.A., Morgan, M.G., Holmes, K.J., 2017. Enhancing the resilience of electricity systems. Engineering 3, 580–582.

Wing, I.S., Rose, A.Z., 2020. Economic Consequence Analysis of Electric Power Infrastructure Disruptions: General Equilibrium Approaches. Energy Economics, 104756.

Wu, H., Xie, Y., Xu, Y., Wu, Q., Yu, C., Sun, J., 2022. Resilient scheduling of MESSs and RCs for distribution system restoration considering the forced cut-off of wind power. Energy 244, 1–14.

Yusta, J.M., Correa, G.J., Lacal-Arántegui, R., 2011. Methodologies and applications for critical infrastructure protection: state-of-the-art. Energy Pol. 39, 6100–6119.

Zhang, B., Xin, Q., Tang, M., Niu, N., Du, H., Chang, X., Wang, Z., 2022a. Revenue allocation for interfirm collaboration on carbon emission reduction: complete information in a big data context. Ann. Oper. Res. 1–24.

Zhang, B., Xin, Q., Tang, M., 2022b. Revenue allocation for interfirm collaboration on carbon emission reduction: complete information in a big data context. Ann. Oper. Res. 2022, 1–24.

Zhang, W., Pei, W., Guo, T., 2014. An efficient method of robustness analysis for power grid under cascading failure. Saf. Sci. 64, 121–126.